

Panax notoginseng saponins ameliorate renal interstitial fibrosis in a rat model of chronic kidney disease via the TLR4/NF- κ B signaling pathway

Xiaodong Zhao¹, Zhenzhen Wang², Hongmei Zhang² and Jianmin Ren^{1*}

¹Department of Endocrinology, Qilu Hospital of Shandong University, Jinan, Shandong, 250012, China

²Department of Endocrinology, Zibo Central Hospital, Zibo, Shandong, 255020, China

Abstract: Background: Renal interstitial fibrosis (RIF) is a core pathological process in the progression of chronic kidney disease (CKD), but effective therapeutic drugs are currently lacking. *Panax notoginseng* saponins (PNS) exhibit potential anti-inflammatory and anti-fibrotic effects, yet their mechanism of action in RIF remains unclear. **Objectives:** This study aims to investigate the ameliorative effects of *Panax notoginseng* saponins (PNS) on renal interstitial fibrosis in a rat model of chronic kidney disease (CKD) and to elucidate whether these effects are mediated through the regulation of the TLR4/NF- κ B signaling pathway. **Methods:** A rat model of CKD was established, with experimental groups including a healthy control group, a model group, PNS-treated group, TAK-242 group, LPS group and combination groups (PNS+TAK-242 and PNS+LPS). Renal pathology and fibrosis were evaluated by HE and Masson staining, while the expression of fibrosis markers and TLR4/NF- κ B pathway molecules was analyzed via RT-qPCR and Western blot. **Results:** (1) Compared with the model group, PNS treatment significantly alleviated renal tissue damage and reduced the fibrotic area, while also downregulating the gene and protein expression of fibrosis markers, TLR4 and Rel (which encodes NF- κ B p65); (2) the TLR4 inhibitor TAK-242 exhibited anti-fibrotic effects similar to those of PNS and the combination of PNS and TAK-242 yielded the most pronounced therapeutic outcomes. **Conclusion:** PNS significantly alleviates renal interstitial fibrosis in the CKD model rats and its mechanism is associated with the inhibition of the TLR4/NF- κ B signaling pathway, thereby downregulating the expression of downstream pro-fibrotic factors.

Keywords: PNS; Renal interstitial fibrosis; TLR4/NF- κ B pathway; TGF- β 1

Submitted on 10-12-2025 – Revised on 30-01-2026 – Accepted on 02-02-2026

INTRODUCTION

Renal interstitial fibrosis (RIF) is a critical pathological process in the progression of chronic kidney disease (CKD) and represents a common endpoint in end-stage renal failure. Currently, CKD affects approximately 10 to 15% of the global population (Bello *et al.*, 2024). RIF lesions are primarily characterized by local deposition of extracellular matrix, loss of peritubular micro vessels and tubular epithelial cells and accumulation of fibroblasts (Zeng *et al.*, 2022). Studies have further demonstrated that the extent of renal interstitial damage correlates with the severity of renal dysfunction across various kidney diseases. Consequently, research on RIF has garnered significant attention in recent decades and has advanced rapidly (Wu *et al.*, 2025). However, the pathogenesis of RIF is highly complex; despite numerous therapeutic approaches, effective and specific treatments for RIF remain lacking. Therefore, there is an urgent need to develop therapeutic strategies with high specificity and minimal side effects.

Traditional Chinese medicine has demonstrated promising efficacy in treating RIF, often with favorable safety profiles and reduced risk of adverse drug reactions or immune rejection (Huang *et al.*, 2025). Thus, identifying traditional Chinese medicinal compounds capable of modulating or

reversing immune dysregulation in CKD is of great research interest. According to the "Compendium of Materia Medica," notoginseng is described as having hemostatic, blood-activating and analgesic properties. *Panax notoginseng* saponins (PNS) are considered the primary active components responsible for its pharmacological effects. PNS exhibit a broad spectrum of therapeutic applications, including vasodilation, which improves local microcirculation and endothelial function, thereby exerting anticoagulant, anti-inflammatory and antioxidant effects. These actions collectively contribute to cardioprotection by reducing myocardial injury (Cui *et al.*, 2024, Xia *et al.*, 2024). PNS can also modulate inflammatory responses by influencing MAPK and related signaling pathways, as well as regulating cytokine levels, T-cell subsets and serum TNF- α , leading to immune regulation (Yang *et al.*, 2025). Furthermore, studies have shown that PNS monomers (Rb1, Rg1, Re) and total saponins possess therapeutic potential in cardiovascular and cerebrovascular diseases, tumors and organ fibrosis (Wu *et al.*, 2024). Nevertheless, the precise mechanism by which PNS ameliorates RIF remains unclear.

Toll-like receptor 4 (TLR4) is a key receptor involved in inflammatory signaling, which activates nuclear factor (NF)- κ B through multiple mechanisms, leading to the widespread expression of inflammatory factors (Yang *et al.*, 2024). Thus, inflammation is largely driven by the

*Corresponding author: e-mail: zz370303@163.com

activation of the TLR4/NF- κ B pathway, along with the overexpression of cytokines such as those associated with the T-helper (TH)1/TH2 response (Yao *et al.*, 2024). These factors collectively contribute to the development of RIF lesions. It has been demonstrated that notoginsenoside R1, a PNS monomer, can suppress the activation of the MAPK signaling pathway (including phosphorylated p65, JNK, ERK and p38), leading to downregulation of downstream gene expression (Yang *et al.*, 2024). Consequently, the anti-inflammatory and antioxidant properties of notoginsenoside R1 are attributed to its ability to inhibit NF- κ B and MAPK pathway activation, thereby reducing fibrogenesis in cells.

Therefore, this study aims to investigate the inhibitory effects of PNS on RIF in a rat model of chronic renal failure, with a focus on the TLR4-mediated NF- κ B signaling pathway, to elucidate the underlying regulatory mechanisms of PNS and explore its potential as an effective therapeutic strategy for RIF. The research framework is illustrated in Fig. 1.

MATERIALS AND METHODS

Experimental animals and reagents

Forty-nine 2-month-old healthy male Sprague-Dawley (SD) rats weighing 220-250 g were purchased from Jiangning Qinglongshan Animal Farm (Nanjing, China).

Drugs and reagents

PNS (Yuanye Company, Shanghai, see fig. 2A for the structure diagram); TLR4 inhibitor group (TAK-242 group, see fig. 2B, for the structure diagram); Fetal bovine serum (Gibco, Thermo Fisher); Biochemical Analysis Kit (Product No. C011-2 and C013-1, Jiancheng Institute of Bioengineering, Nanjing) ELISA Kit (R&D Company); TRizol Reagent, α -SMA (1:1 000, Bobst Biotechnology LTD, Wuhan), RT-PCR kit (Bao Biotech LTD, Dalian); Masson staining kit (China Biotech LTD; Wuhan); GAPDH (1:5 000, Protein Technology Group); Optical microscope (Nikon); All author reagents were domestically produced and purified.

Experimental method

Animal model preparation

A chronic renal failure (CRF) rat model was established using the 5/6 nephrectomy method as previously described (Hashimoto *et al.*, 2022). Rats were housed under standard conditions at 21 \pm 2 $^{\circ}$ C with free access to food and water and a 12-h light/dark cycle. After 7 days of acclimatization, surgery was performed on day 8. Briefly, rats were anesthetized via intraperitoneal injection of pentobarbital sodium (45 mg/kg). The right kidney area was shaved and disinfected, followed by a skin incision to expose the kidney. The renal capsule was carefully removed and approximately two-thirds of the right kidney (upper and lower poles) was excised. Hemostasis was achieved and the kidney remnant was returned to the abdominal cavity,

followed by layered suturing. Seven days later, the left renal pedicle was ligated and the left kidney was completely removed.

Animal grouping and intervention

Rats were randomly divided into seven groups (n=5 per group): Healthy control group (normal rats), Model group (CRF rats without treatment), PNS group (CRF rats treated with PNS), TAK-242 group (CRF rats treated with TLR4 inhibitor TAK-242), LPS group (CRF rats treated with TLR4 activator LPS), PNS + TAK-242 group (CRF rats treated with PNS and TAK-242), PNS + LPS group (CRF rats treated with PNS and LPS).

Treatments were administered as follows: TAK-242 group: rats with renal failure models were intraperitoneally injected with TAK-242 (dose: 3 mg/kg, once daily for 4 weeks) (Li *et al.*, 2019); LPS group: rats with renal failure models were intraperitoneally injected with LPS (dose: 1 mg/kg, twice weekly for 4 weeks; determined based on preliminary experiments to activate TLR4 signaling without inducing significant systemic inflammatory responses or multi-organ damage, with monitoring of the general condition of animals and serum inflammatory factor levels during the experiment); PNS group: rats were orally administered PNS (dose: 100 mg/kg, once daily for 4 weeks) (Hu *et al.*, 2018); PNS + TAK-242 group and PNS + LPS group: rats with renal failure models were treated with PNS combined with TAK-242 or LPS, respectively, using the same administration routes and doses as in the single-treatment groups.

Determination of biochemical index levels in rats

Seven days after the completion of modeling, blood samples were collected from the retro-orbital plexus of rats under light anesthesia. Serum creatinine (Scr) and blood urea nitrogen (BUN) levels were measured using commercial assay kits to confirm successful induction of renal impairment (Huang *et al.*, 2026).

Pathological features detected by HE staining

Renal tissues were fixed in formaldehyde, dehydrated through a graded ethanol series and embedded in paraffin. Sections (5 μ m thick) were stained with hematoxylin and eosin (HE). Histopathological changes were examined under a light microscope at 400 \times magnification (Nikon, model eclipse E400). Ten fields per section were randomly selected in a blinded manner. Five cells per field with distinct nuclei and clear cytoplasmic staining were analyzed. The average cell area and equivalent circular diameter were measured using Image-Pro Plus software and the mean transverse diameter of myocytes was recorded (Li *et al.*, 2025).

Masson staining to detect the degree of tissue fibrosis

Paraffin-embedded renal sections were dewaxed, rehydrated and stained using a Masson trichrome staining kit according to the manufacturer's instructions. Briefly,

sections were stained with iron hematoxylin, differentiated in 1% acid alcohol, incubated in ponceau-acid fuchsin, treated with 1% phosphomolybdic acid for 5 min, counterstained with aniline blue for 5 min and rinsed in 1% acetic acid. Slides were then dehydrated and mounted. Collagen fibers appeared blue, muscle fibers red and erythrocytes bright red. Five randomly selected fields per section were examined under a light microscope (Nikon, model eclipse E400). The percentage of fibrotic area was quantified using image analysis software as follows: RIF area percentage (%) = positive staining area/field of view × 100% (van de Vlekkert *et al.*, 2020).

Western blot

The BCA method was used to quantitatively analyze the protein content of kidney cells in each group. After loading 10 µL of sample solution and protein standard per well, polyacrylamide gel electrophoresis was performed under the following conditions: stacking gel at 80 V for 30 min and separating gel at 120 V until the bromophenol blue reached the bottom of the gel. Proteins were transferred onto a PVDF membrane using the wet transfer method under conditions of 300 mA for 90 min. Blocking was carried out with 5% skimmed milk (prepared with TBST) at room temperature for 1 hour. Primary antibodies (TLR4, 1:1000; NF-κB p65, 1:1000; GAPDH, 1:5000) were incubated overnight on a shaker at 4°C. The secondary antibody (horseradish peroxidase-labeled, 1:5000) was incubated at room temperature for 1 hour. After ECL development, grayscale analysis was performed using ImageJ software.

Real-time quantitative PCR (RT-qPCR)

Total RNA (1 µg) was taken and the concentration and purity were measured using a NanoDrop 2000 spectrophotometer (Thermo Fisher Scientific), with A260/A280 ratios ranging between 1.8 and 2.0. Reverse transcription was performed using the PrimeScript RT reagent Kit with a reaction volume of 20 µL, strictly following the manufacturer's instructions. Real-time fluorescence quantitative PCR was conducted using the SYBR Green method on an ABI 7500 Fast system. The reaction mixture (20 µL) consisted of 10 µL of SYBR Premix Ex Taq II (2×), 0.8 µL each of forward and reverse primers (10 µM), 2 µL of cDNA template and 6.4 µL of sterile water. PCR conditions were as follows: pre-denaturation at 95°C for 30 s; 40 cycles of 95°C for 5 s and 60°C for 30 s; followed by melt curve analysis. Three technical replicates were performed for each sample. Ct values were recorded and the $2^{-\Delta\Delta Ct}$ method was used to calculate the relative expression levels of target genes normalized to the internal reference gene β-actin (Rao *et al.*, 2013). The primer sequences are listed in table 1.

Statistical analysis

Statistical analyses were performed using SPSS 21.0 and GraphPad Prism. Data are presented as mean ± SD.

Normality and homogeneity of variance were confirmed. One-way ANOVA followed by the LSD post hoc test was used for group comparisons. A P value < 0.05 was considered statistically significant.

RESULTS

Construction of rat renal failure model and determination of biochemical index levels

Biochemical analysis revealed that serum creatinine (Scr) and blood urea nitrogen (BUN) levels were significantly elevated in model rats compared with healthy controls (P < 0.001; Figs. 3A and B), confirming successful induction of chronic kidney disease. General condition observations indicated that healthy rats exhibited normal mental status, responsiveness, feeding, drinking, defecation and smooth, shiny fur. In contrast, renal failure model rats displayed varying degrees of mental depression, reduced responsiveness, decreased food and water intake, weight loss and markedly reduced activity. Their fur appeared dull, prone to shedding and they often exhibited hunched posture and piloerection.

PNS significantly inhibited the changes of renal interstitial fibrosis through downregulation of TLR4 and NF-κB p65

HE and Masson staining of kidney tissues from the three groups revealed distinct pathological features. Healthy control rats showed normal renal architecture with no apparent damage or inflammation. In contrast, model group rats exhibited tubular dilation, luminal crystalline deposits, extensive interstitial fibrosis, hyperplasia and significant inflammatory cell infiltration. PNS treatment markedly reduced fibrotic area and inflammatory infiltration compared with the model group (Fig. 4A).

PNS intervention significantly downregulated the mRNA expression of fibrosis markers, including TGF-β1, α-SMA, collagen I and FN (VS model group, P<0.05, Figs. 4B, 4C, 4D and 4E). Furthermore, both gene and protein expression levels of TLR4 and NF-κB p65 were elevated in model rats but significantly reduced following PNS treatment (Figs. 4F, 4G and 4H). These consistent reductions suggest that the anti-fibrotic effects of PNS are associated with suppression of the TLR4/NF-κB signaling pathway.

PNS can inhibit the expression of TLR4 and after using TAK-242, the expressions of TGF-β1, α-SMA, collagen I and FN in kidney cells are down-regulated and the PNS + TAK-242 group is the most significant

To further investigate the role of the TLR4/NF-κB pathway in RIF, additional groups treated with the TLR4 inhibitor TAK-242 or activator LPS were included. LPS treatment significantly upregulated the expression of TGF-β1 (Fig. 5A), α-SMA (Fig. 5B), collagen I (Fig. 5C) and FN (Fig. 5D) compared with the model group (P < 0.05), whereas TAK-242 treatment downregulated these markers.

Table 1: Primer sequences.

Gene	Primer	Sequences
TLR4	Forward	5'-GTTTGACATTGCTCGGTCCT-3'
	Reverse	5'-CCTCCTCAGATATCGGGACA-3'
NF- κ B p65 (RELA)	Forward	5'-TCAACGCAGGACCTAAAGACAT-3'
	Reverse	5'-GCAGATAGCCAAGTTCAGGATG-3'
TGF- β 1	Forward	5'-ATGAACCGACCCTTCCTGCT-3'
	Reverse	5'-CCTGGTTGTGTTGGTTGTAGAG-3'
α -SMA	Forward	5'-AGCCAGTCGCCATCAGGAAC-3'
	Reverse	5'-CCGGAGCCATTGTCACACAC-3'
Collagen I	Forward	5'-GAGAGAGCATGACCGATGGA-3'
	Reverse	5'-CGTGCTGTAGGTGAATCGAC-3'
FN	Forward	5'-AACGGCCCTGGTTTGTACC-3'
	Reverse	5'-CTCCAACATATAGCCACCAGTC-3'
β -actin	Forward	5'-CAGGAGGCATTGCTGATGAT-3'
	Reverse	5'-GAAGGCTGGGCTCATT-3'

*NF- κ B is a transcription factor complex. In this study, the mRNA expression of its subunit RELA (encoding the p65 protein) was detected

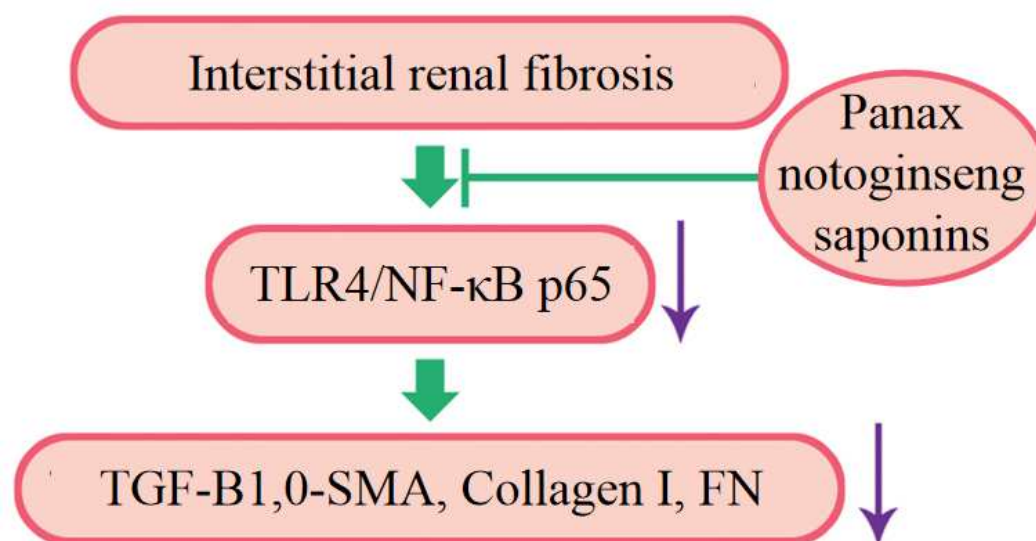


Fig. 1: PNS consistent with TLR4/NF- κ B p65 pathway activity and then down-regulate the expression of TGF- β 1, α -SMA, collagen I and FN; and reduce the degree of fibrosis.

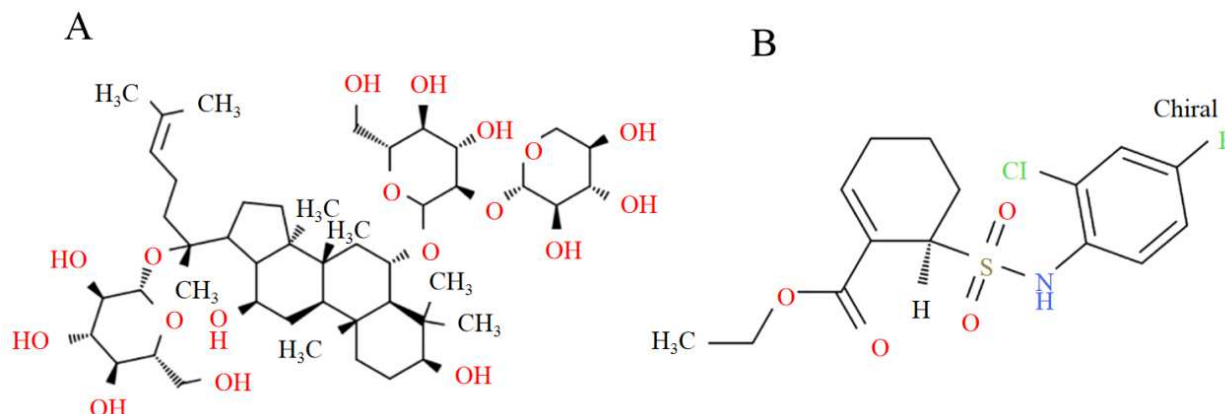


Fig. 2: Structural diagram of PNS and TLR4 inhibitors. (A) The structural diagram of PNS; (B) The structural diagram of TLR4 inhibitors.

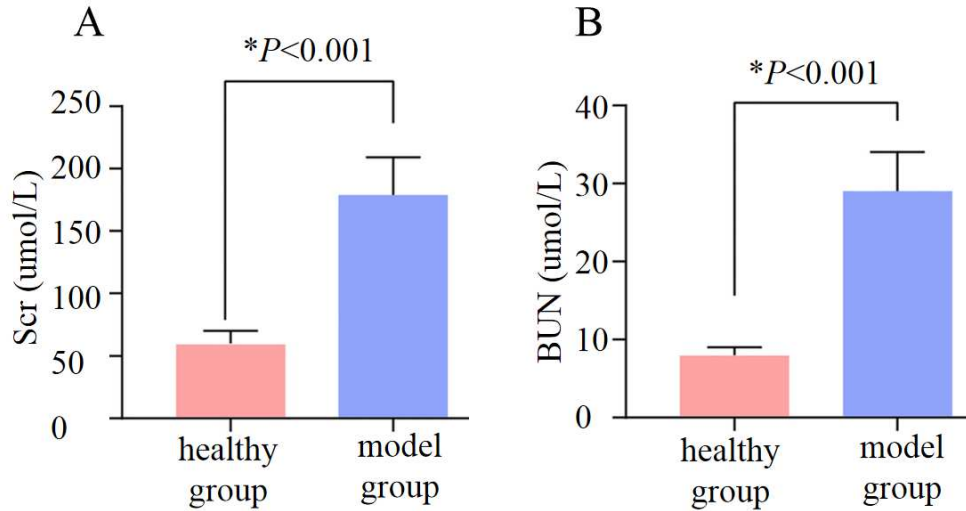


Fig. 3: Detection results of biochemical indicators in two groups of rats. (A) Scr levels of two groups of rats; (B) BUN levels of two groups of rats; n=5.

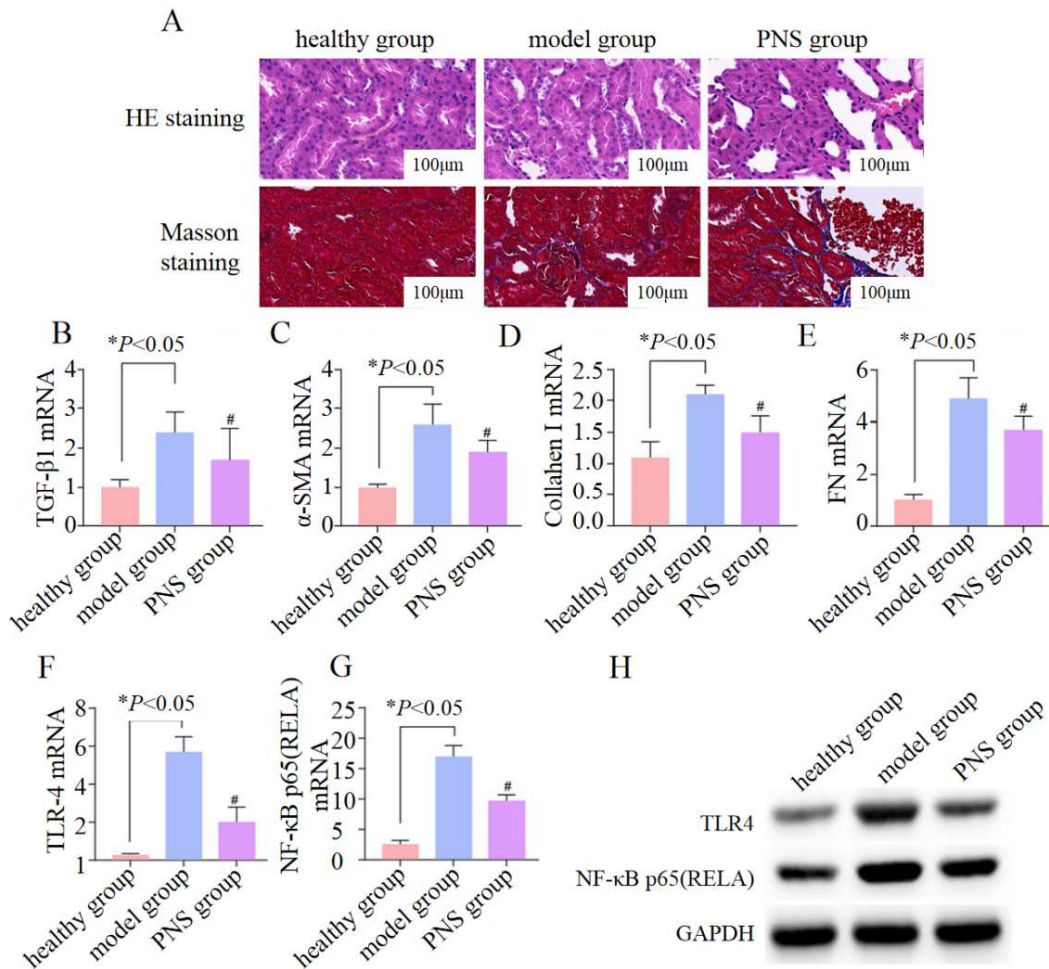


Fig. 4: The effect of PNS on renal tissue fibrosis. (A) HE staining and Masson staining to observe the degree of renal tissue fibrosis (×200); (B) PCR detection of TGF-β1 expression; (C) PCR detection of α-SMA expression; (D) PCR detection of collagen I expression; (E) PCR detection of FN expression; (F) PCR detection of TLR4 expression; (G) PCR detection of NF-κB p65(RELA) mRNA expression; (H) Western blot detection of TLR4 and NF-κB protein expression; compared with the model group, #P<0.05, n=5.

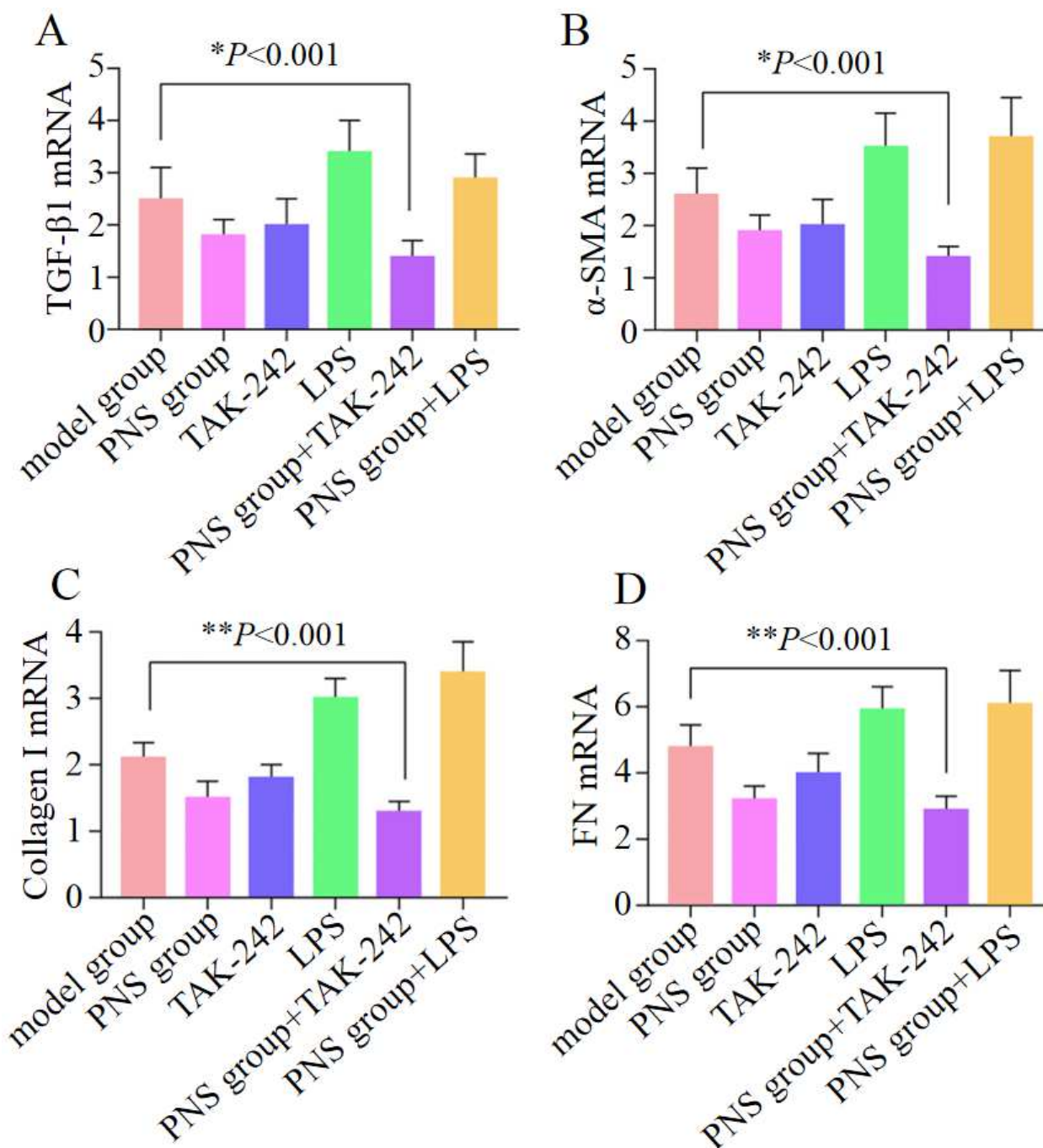


Fig. 5: Effect of PNS on renal tissue fibrosis through TLR4/NF- κ B pathway. (A) PCR detection of TGF- β 1 expression; (B) PCR detection of α -SMA expression; (C) PCR detection of collagen I expression; (D) PCR detection of FN expression; n=5.

Notably, the anti-fibrotic effects of TAK-242 were comparable to those of PNS ($P > 0.05$ between groups), suggesting that PNS may inhibit RIF through a mechanism involving TLR4 down regulation.

The LPS dose used was optimized to selectively activate TLR4 signaling without inducing systemic inflammation or direct renal injury, confirming that the observed pro-fibrotic effects were pathway-specific.

To explore the interaction between PNS and TLR4, a combined treatment group (PNS + TAK-242) was examined. This combination (PNS + TAK-242) resulted in the most pronounced reduction in TGF- β 1, α -SMA, collagen I and FN expression ($P < 0.05$ vs. all other groups; Fig. 5A-D), indicating that PNS exerts potent anti-fibrotic effects under conditions of TLR4 inhibition.

DISCUSSION

The association between fibrosis and inflammation is well-established and supported by morphological evidence. Inflammation plays an essential role in the progression of renal interstitial fibrosis (RIF), as demonstrated in numerous clinical studies (Chen *et al.*, 2023). Toll-like receptors (TLRs), as innate immune receptors, recognize endogenous risk factors in RIF and contribute to the activation of immune and inflammatory responses. A previous study (Li *et al.*, 2023) reported that impaired renal function in mouse models is associated with extensive extracellular matrix accumulation and overexpression of epithelial-mesenchymal transition markers in HK-2 cells. Therefore, a promising therapeutic strategy for RIF involves identifying traditional Chinese medicinal compounds that can effectively inhibit inflammatory factor production or suppress the TLR4/NF- κ B signaling pathway. Furthermore, A previous study (Li *et al.*, 2024) demonstrated that PNS effectively attenuates pulmonary fibrosis in rat models, suggesting their broad anti-fibrotic potential. These findings indicate that PNS may serve as a promising candidate for treating RIF. As a component of traditional Chinese medicine, PNS are generally associated with low immunogenicity and reduced risk of immune rejection. In patients with specific constitutions, PNS may offer unique therapeutic benefits (Jiang *et al.*, 2022, Zhou *et al.*, 2024). Building on previous research, the present study successfully established a rat model of renal failure and investigated the effects of PNS on fibrosis-related gene expression to elucidate its mechanism in RIF treatment. PNS are known to exert anticoagulant, anti-inflammatory and antioxidant effects, while also preserving vascular elasticity, ameliorating endothelial injury and improving microcirculation (Wang *et al.*, 2024). Existing evidence suggests that PNS reduces inflammatory factor production by modulating MAPK-related signaling pathways and regulating cytokine synthesis and apoptosis (Li *et al.*, 2022). Nevertheless, the precise mechanism by which PNS ameliorates RIF *in-vivo* remains unclear.

A previous study (Ram *et al.*, 2022) reported that biochanin A (BCA) inhibits renal fibroblast gene expression by attenuating receptor activation and ameliorates RIF through suppression of the NF- κ B/NLRP3 signaling pathways. These findings highlight the role of NF- κ B-mediated fibroblast activation in kidney disease progression. Similarly, a previous study (Wang *et al.*, 2024) demonstrated that PNS can inhibit the NF- κ B pathway by preventing the phosphorylation of NF- κ B inhibitors, further supporting the involvement of this pathway in fibrosis regulation. Collectively, these results suggest that PNS exert therapeutic effects by inhibiting the TLR4/NF- κ B signaling pathway, thereby reducing the overexpression of downstream pro-fibrotic genes. The current study initially compared the normal control, model and PNS-treated groups to evaluate whether PNS inhibits,

promotes, or has minimal effect on RIF. Data analysis revealed that PNS treatment significantly down regulated TGF- β 1, α -SMA, collagen I and FN expression compared with the model group, accompanied by reduced TLR4/NF- κ B pathway activity. These findings are consistent with prior research (Yi *et al.*, 2025) and indicate a strong association between the anti-fibrotic effects of PNS and suppression of the TLR4/NF- κ B pathway.

Subsequent comparisons among the model, PNS, TAK-242, LPS, PNS + TAK-242 and PNS + LPS groups revealed that the PNS + TAK-242 combination exerted the most potent anti-fibrotic effect, whereas the LPS group showed the worst outcomes. This further supports the notion that PNS inhibits RIF primarily through suppression of NF- κ B signaling. Mechanistically, PNS may downregulate TLR4 expression, leading to NF- κ B inhibition, which in turn reduces TGF- β 1 levels and attenuates renal tubular epithelial cell trans differentiation and mesenchymal transition (Xin *et al.*, 2026). As a key biomarker of fibrosis, α -SMA (Tian *et al.*, 2021) and collagen I, a major contributor to RIF (Imai *et al.*, 2023), were both downregulated following PNS treatment. Thus, PNS-mediated inhibition of the TLR4/NF- κ B pathway results in decreased expression of TGF- β 1, α -SMA and collagen I, collectively ameliorating RIF (Yuan *et al.*, 2022). While previous research has predominantly focused on cardiovascular and cerebrovascular diseases, examining the role of the TLR4/NF- κ B pathway in inflammatory responses within those contexts, the present study demonstrates that PNS attenuates chronic kidney disease progression in rats by inhibiting NF- κ B signaling. These findings help address a gap in prior clinical and experimental research on renal fibrosis.

CONCLUSION

In summary, PNS significantly inhibits renal fibrosis by suppressing the TLR4/NF- κ B signaling pathway and downregulating the expression of fibrosis-related factors such as TGF- β 1 and α -SMA. However, this study was conducted only at the cellular and animal levels and PNS has not yet been evaluated in clinical trials for the treatment of RIF. Therefore, further studies are needed to assess the regulatory mechanisms of PNS in patients with renal failure.

Acknowledgments

Not applicable.

Authors' contribution

Jianmin Ren: Responsible for experimental design and execution, data collection, statistical analysis and drafting of the initial manuscript; Xiaodong Zhao: Participated in animal experiments, sample processing, pathological analysis and data organization; Zhenzhen Wang: Proposed the research concept, secured funding and supervised the

entire project; Hongmei Zhang: Performed data analysis and interpretation and conducted the final review and approval of the manuscript.

Funding

This work was supported by The Shandong Province Medical Health Science and Technology Project (202303060681) and Zibo Medical and Health Research Project (20230306020).

Data availability statement

The datasets generated and/or analyzed during the current study are available from the corresponding author on reasonable request.

Ethical approval

This study was approved by the ethnic committee of Zibo Central Hospital (2023059).

Conflict of interest

The authors declare that this research was conducted without any commercial or financial interests that could be interpreted as potential conflicts of interest.

REFERENCES

- Bello AK, Okpechi IG, Levin A, Ye F, Damster S, Arruebo S, Donner JA, Caskey FJ, Cho Y, Davids MR, Davison SN, Htay H, Jha V, Lalji R, Malik C, Nangaku M, See E, Sozio SM, Tonelli M, Wainstein M, Yeung EK, Johnson DW and Group IG (2024). An update on the global disparities in kidney disease burden and care across world countries and regions. *Lancet Glob Health*, **12**(3): e382-e395.
- Chen W, Zhao S, Xing J, Yu W, Rao T, Zhou X, Ruan Y, Li S, Xia Y, Song T, Zou F, Li W and Cheng F (2023). BMAL1 inhibits renal fibrosis and renal interstitial inflammation by targeting the ERK1/2/ELK-1/Egr-1 axis. *Int Immunopharmacol.*, **125**(Pt B): 111140.
- Cui XH, Zhang L, Lin L, Hu YL, Zhang MX, Sun BW, Zhang ZY, Lu MK, Guan XY, Hao JQ, Li YL and Li C (2024). Notoginsenoside R1-Protocatechuic aldehyde reduces vascular inflammation and calcification through increasing the release of nitric oxide to inhibit TGF β R1-YAP/TAZ pathway in vascular smooth muscle cells. *International Immunopharmacology*, **143**: 113574.
- Hashimoto A, Gao JQ, Kanome Y, Ogawa Y, Nakatsu M, Kohno M and Fukui K (2022). Evaluation of cerium oxide as a phosphate binder using 5/6 nephrectomy model rat. *BMC Nephrology*, **23**(1): 277.
- Hu SN, Wu YL, Zhao B, Hu HY, Zhu BC, Sun ZX, Li PY and Du SY (2018). Saponins protect cerebral microvascular endothelial cells against oxygen-glucose deprivation/reperfusion-induced barrier dysfunction via activation of PI3K/Akt/Nrf2 antioxidant signaling pathway. *Mol.*, **23**(11): 2781.
- Huang J, Fu Y, Fu Y, Pan Y, Hu Y, Zhang J, Guo W and Du X (2026). Associations of serum creatinine and blood urea nitrogen with depressive symptoms among community-dwelling older adults in Guangzhou, China: A cross-sectional study. *Front Psychiatry*, **17**: 1746646.
- Huang SY, Wang XX, Chen GT, Chen KL, Chen X and Zhang LQ (2025). Prevention and treatment of acute kidney injury, renal interstitial fibrosis and diabetic kidney disease by regulating endoplasmic reticulum stress with traditional Chinese medicine: A review. *Zhongguo Zhong Yao Za Zhi*, **50**(22): 6227-6233.
- Imai K, Ishimoto T, Doke T, Tsuboi T, Watanabe Y, Katsushima K, Suzuki M, Oishi H, Furuhashi K, Ito Y, Kondo Y and Maruyama S (2023). Long non-coding RNA lnc-CHAF1B-3 promotes renal interstitial fibrosis by regulating EMT-related genes in renal proximal tubular cells. *Mol Ther Nucleic Acids*, **31**: 139-150.
- Jiang Y, Li H, Huang P, Li S, Li B, Huo L, Zhong J, Pan Z, Li Y and Xia X (2022). *Panax notoginseng* saponins protect PC12 cells against Abeta induced injury via promoting parkin-mediated mitophagy. *J Ethnopharmacol.*, **285**: 114859.
- Li H, Wang YG, Chen TF, Gao YH, Song L, Yang YF, Gao Y, Huo W and Zhang GP (2024). *Panax notoginseng* saponin alleviates pulmonary fibrosis in rats by modulating the renin-angiotensin system. *J Ethnopharmacol.*, **318**(Pt B): 116979.
- Li H, Zhu J, Xu YW, Mou FF, Shan XL, Wang QL, Liu BN, Ning K, Liu JJ, Wang YC, Mi JX, Wei XH, Shao SJ, Cui GH, Lu R and Guo HD (2022). Notoginsenoside R1-loaded mesoporous silica nanoparticles targeting the site of injury through inflammatory cells improves heart repair after myocardial infarction. *Redox Biol.*, **54**: 102384.
- Li R, Guo YJ, Zhang YM, Zhang X, Zhu LP and Yan TH (2019). Salidroside ameliorates renal interstitial fibrosis by inhibiting the TLR4/NF-B and MAPK signaling pathways. *Inter J. Mol. Sci.*, **20**(5): 1103.
- Li X, Dong W, Yang Y, Ren S, Wang X, Zou M, Lu W, Liu L and Xue Y (2023). Ecliptasaponin A attenuates renal fibrosis by regulating the extracellular matrix of renal tubular cells. *In vitro Cell Dev Biol Anim.*, **59**(9): 684-696.
- Li Z, Sun X, Wang Y, Zhang F, Wang L, Ai C, Zhang X, Yin X, Liu C, Li C and Lu C (2025). Renal denervation attenuates cardiac dysfunction in HFpEF by inhibiting the ATP-P2X7-NLRP3 inflammasome axis. *Basic Res Cardiol*, **120**(6): 1225-1247.
- Ram C, Gairola S, Syed A, Kulhari U, Kundu S, Mugale MN, Murty US and Sahu BD (2022). Biochanin A alleviates unilateral ureteral obstruction-induced renal interstitial fibrosis and inflammation by inhibiting the TGF- β 1/Smad2/3 and NF-kB/NLRP3 signaling axis in mice. *Life Sci*, **298**: 120527.
- Rao X, Huang X, Zhou Z and Lin X (2013). An improvement of the 2⁻(-delta delta CT) method for quantitative real-time polymerase chain reaction data analysis. *Biostat Bioinforma Biomath.*, **3**(3): 71-85.

- Tian J, Xiao Z, Ju W, Shan Y, Zeng D, Tao YL, Fang X, Tang CY, Chen XJ and Li Y (2021). NCTD prevents renal interstitial fibrosis via targeting Sp1/lncRNA Gm26669 axis. *Int J Bio Sci*, **17**(12): 3118-3132.
- Van de Vlekkert D, Machado E and d'Azzo A (2020). Analysis of generalized fibrosis in mouse tissue sections with masson's trichrome staining. *Bio-Protocol*, **10**(10): e3629-e3629.
- Wang Y, Sun X, Xie Y, Du A, Chen M, Lai S, Wei X, Ji L and Wang C (2024). *Panax notoginseng* saponins alleviate diabetic retinopathy by inhibiting retinal inflammation: Association with the NF-kappaB signaling pathway. *J Ethnopharmacol.*, **319**(Pt 1): 117135.
- Wu JJ, Zhang L, Liu D, Xia J, Yang Y, Tang F, Chen L, Ao H and Peng C (2024). Ginsenoside Rg1, lights up the way for the potential prevention of Alzheimer's disease due to its therapeutic effects on the drug-controllable risk factors of Alzheimer's disease. *J. Ethnopharmacol.*, **318**: 116955.
- Wu S, Guo ML, Wang YD, Zhou YL, Zhang LY, Zhou Y, Xing YY, Sun D, Hu XQ, Ruan ZM, He JCJ and Ren HQ (2025). Relationship between podocyte injury and renal outcomes in patients with acute kidney injury: A report from a retrospective study in China. *Am. J. Nephrol.*, **56**(5): 595-604.
- Xia JY, Chen C, Sun YN, Li SA, Li YX, Cheng BR, Pang YT, Li Y, Li D and Lin Q (2024). *Panax quinquefolius* saponins and *Panax notoginseng* saponins attenuate myocardial hypoxia-reoxygenation injury by reducing excessive mitophagy. *Cell Biochem Biophys*, **82**(2): 1179-1191.
- Xin L, Kanghao N, Jiacheng L, Xiaodong Y, Juhan Y, Xinyang Z and Xiangdong L (2026). *Panax notoginseng* saponins inhibit apoptosis and alleviate renal ischemia-reperfusion injury through the ROCK2/NF-kappaB pathway. *Mol Biotechnol.*, **68**(1): 223-234.
- Yang J, Zhang MX, Luo YM, Xu F, Gao F, Sun YP, Yang BY and Kuang HX (2024). Protopine ameliorates OVA-induced asthma through modulating TLR4/ MyD88/NF-κB pathway and NLRP3 inflammasome-mediated pyroptosis. *Phytomedicine*, **126**: 154410.
- Yang X, Wu TT, Zhu HP, Ding HY, Chen X, Xu QF, Sun HW and Liang GQ (2025). *Panax notoginseng*-*Bletilla striata* ameliorates reflux esophagitis by modulating NLRP3 inflammasomes and p38 MAPK pathway. *Cytotech.*, **78**(1): 3.
- Yao Q, Lin DM, Yang YY and Zhuang YH (2024). Combination of doxycycline with metronidazole protects against pyroptosis in rats with endometritis through the modulation of pathway. *Discov. Med.*, **36**(180): 140-149.
- Yi S, Li FY, Ma X, Xu Y, Lai WJ, Chen HX, Fan JM, Mao N and Ren SC (2025). Panaxatriol saponins exert anti-renal fibrosis by suppressing TNF-α mediated inflammation and TGF-β1/Smad3 signaling pathway. *Ren Fail.*, **47**(1): 2516774.
- Yuan Y, Liu YX, Sun MY, Ye HJ, Feng YC, Liu ZZ, Pan LY and Weng HB (2022). Aggravated renal fibrosis is positively associated with the activation of HMGB1-TLR2/4 signaling in STZ-induced diabetic mice. *Open Life Sci.*, **17**(1): 1451-1461.
- Zeng H, Gao Y, Yu W, Liu J, Zhong C, Su X, Wen S and Liang H (2022). Pharmacological inhibition of STING/TBK1 signaling attenuates myeloid fibroblast activation and macrophage to myofibroblast transition in renal fibrosis. *Front Pharmacol.*, **13**: 940716.
- Zhou R, Zhang J, Zhang W, Zhang X, Zhang H, Shi X, Wang B, Zhang Q and Zhang H (2024). Clinical efficacy and safety of *Panax notoginseng* saponins in treating chronic obstructive pulmonary disease with blood hypercoagulability: A meta-analysis of randomized controlled trials. *Phytomed.*, **125**: 155244.